SOLAR ROTATION VELOCITY DETERMINED BY CORONAL BRIGHT POINTS - NEW DATA AND ANALYSIS

M. MULEC[1], R. BRAJŠA[2], H. WÖHL[3], A. HANSLMEIER[1],
B. VRŠNAK[2], V. RUŽDJAK[2], J.-F. HOCHEDEZ[4] and J. ENGLER[5] *

[1]*Institute of Physics, IGAM, University of Graz, Graz, Austria*
[2]*Hvar Observatory, University of Zagreb, Zagreb, Croatia*
[3]*Kiepenheuer-Institut für Sonnenphysik (KIS), Freiburg, Germany*
[4]*Royal Observatory of Belgium, Bruxelles, Belgium*
[5]*University of Konstanz, Konstanz, Germany*

Abstract. Full-disc solar images obtained with the Extreme Ultraviolet Imaging Telescope on board the Solar and Heliospheric Observatory were used to analyse solar differential rotation determined by tracing coronal bright points. Rotation velocity residuals, meridional motions and their relationship are investigated for a new data set from October 1, 1999 to March 31, 2000. Further we take care for the evolution of the single structures, dividing them into Point-Like-Structures, Small Loops and Small Active Regions and analysing their variation in intensity and size.

Key words: solar differential rotation - coronal bright points - evolution

1. Introduction

Coronal bright points (CBPs) proved to be a very useful tool to investigate the dynamics of the solar corona. Especially their role as tracers to make conclusions about the differential rotation of the Sun (Brajša et $al.$, 2002; Vršnak et $al.$, 2003) is important. With a spatial scale of 5 - 25 Mm, a total energy-release of 10^{26}erg to 10^{28}erg and lifetimes from few hours to several days, the CBPs can be observed at EUV wavelengths in EIT-images. The main advantage in comparison to sunspots is, that CBPs are well distributed all over the solar surface, even in polar regions where sunspots do not appear.

In the present paper results for a new set of EIT-images taken in October 1999 are analysed in the same way as in Brajša et $al.$ (2002) for previous

---

*research student at KIS on leave from University of Konstanz

CBPs observations. The motion of bright points was followed over their whole lifetime by using the interactive method to pick CBPs out of EIT-images as in Brajša *et al.* (2001). From that we get results for rotational and meridional motion, changes in size and intensity. The results are displayed and compared to the automatic method by which Wöhl *et al.* (2001) and Brajša *et al.* (2002) analysed the solar rotation and CBP-motion for older data sets.

In this work a more detailed analysis of size- and intensity-variations of coronal bright points is performed. The correlations of changes in radius and intensity are the subject of research taking into account the different tracer types, which are defined due to their individual appearances. Additionally, the question whether or not the growth of bright points might be correlated with the effect of the visible diameter-stretching by the passage over the solar disc, i.e., by change of the central meridian distance (CMD), is investigated.

2. Data and Methods

For the tracing of coronal bright points the Extreme Ultraviolet Imaging Telescope (EIT) on board the Solar and Heliospheric Observatory (SOHO) spacecraft delivers very useful full-disc solar images in Fe XV at 28.4 nm wavelength as in Figure 1. The images are taken 4 times a day every 6 hours. So far two series of images were taken from SOHO in total, as shown in Table I. Rotational and meridional motions have been analysed by 7 observers for the first and by 4 observers for the second series. These observations were

Table I: Two data-sets

Series 1	Series 2
The first data-set covers the time between June '98 until May '99. It consists of 463 images taken in June, November, December '98, March, April and May '99.	The second set spans over 6 months from October '99 to March 2000. 638 images set a much more continuous series with much fewer and shorter gaps.
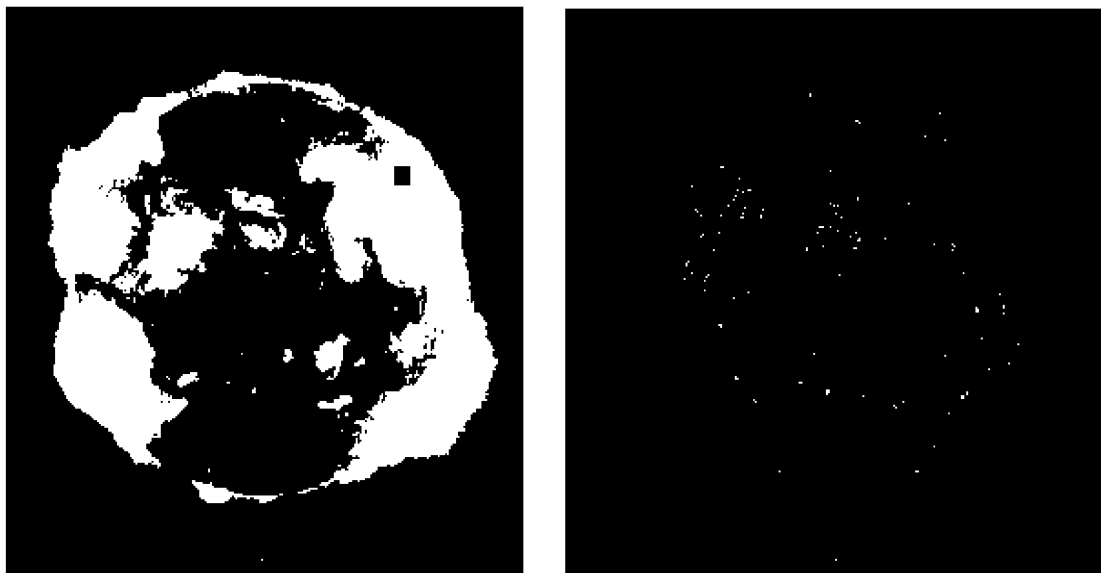
Figure 1: left: EIT-image. Outside the active regions small coronal structures can be seen and easily followed in consecutive images. right: Regions Of Interest (ROI) picked out by the automatic method from the EIT-image on the left. The image was taken on October 1, 1999, 01:07:17 UT

made using a set of programs written in the Interactive Data Language (IDL); an observer follows the motion of a point over its whole life-period, and for every image, the position (solar latitude, CMD), intensity, size in pixels and date of measurement are stored in a sample file for each bright point (interactive method).

The automatic method is independent from physical observers, features declared as IDL Regions Of Interest (ROI) are picked out of the EIT-images as in Figure 1. Always triplets of consecutive images are treated, in which the point's motion is followed. The coordinates of individual points are stored automatically what providing a much faster and non-subjective detection compared to the interactive one. Out of the stored properties, for each identified tracer the prevailing subtype is determined (only for the interactive method), and meridional and rotational angular velocities with errors and average positions are calculated. The new analysis was made by the interactive method for 160 features from the Series 2 in October 1999 and compared to results of other observers, which analysed the October 1999 data, and to the results obtained by the automatic method for both data-series.

3.   Results for the Rotation Velocities

As mentioned above, CBPs were followed over consecutive images in intervals of 6 hours. From this propagation in the observed time over the solar disc the rotational and meridional angular velocity could be computed, using the solar latitude b and CMD as coordinates. For all values of the rotational angular velocity the following fit is used to describe the average differential rotation of the Sun:

$$\omega\left(b\right) = A + B\sin^2\left(b\right) + C\sin^4\left(b\right) \tag{1}$$

In equation (1) A, B and C are constants, b is the solar latitude in degrees and $\omega\left(b\right)$ is the rotational angular velocity. With the substitution $x = \sin^2(b)$ and the measured values $y = \omega\left(b\right)$ we computed a polynomial-fit of rank 2.

We treated both hemispheres together and for an easier comparison with other results (fits), the constant C was put to $C = 0$, generating a linear fit. For 160 features in October 1999, observer M.Mulec :

- The fit for ω_{rot} where $x = \sin^2\left(b\right)$ gives values
  $A = 14.43$ $B = -0.76$ $C = -3.3$

- The fit with $C = 0$ presented in Figure 3 shows
  $A = 14.619 \pm 0.11$ $B = -3.194 \pm 0.31$ in 8-18°
  $A = 14.662 \pm 0.086$ $B = -3.11 \pm 0.249$ with 2°-belt

As presented in Figure 2, the fits are showing nearly the same behaviour and differ only for higher latitudes, what might be caused by the lack of data for b higher than 70°.

To scale down the effect of modifying the fit by points lying too far away from the average value, the data has to be filtered. Figure 3 shows results for the rotational angular velocity using filtered data. The data set observed by M.Mulec consists of 160 features in October 1999 and was filtered in two steps: First, points lying too far away from the average were excluded, so that they can not falsify the fit too much. According to Brajša *et al.* (2002) this seems to be appropriate for CBPs with $\omega_{rot} \geq 18\frac{deg}{day}$ and $\omega_{rot} \leq 8\frac{deg}{day}$. So only points lying inside this interval were used. The second step was an adaptive kind of filtering; we used a preliminary fit computed from data filtered by the first step, then we put a $\pm 2°$-belt around the fit to exclude
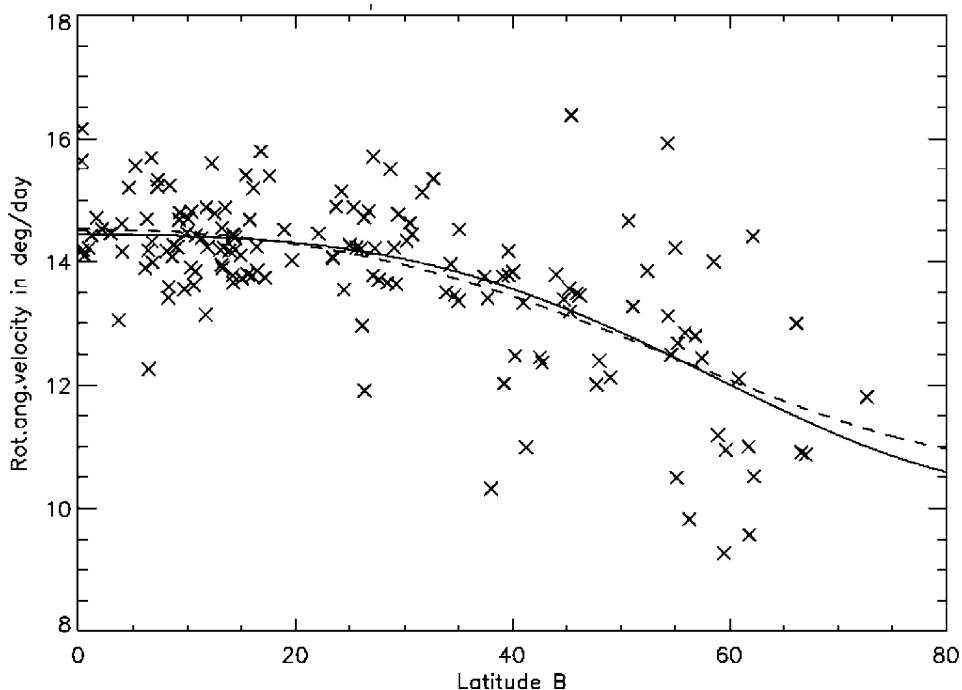
Figure 2: Comparison between two possible fits for 160 features in October 1999. Dashed line: Fit for $C = 0$. Full line: Fit for $C \neq 0$. Both fits show nearly the same behaviour, except for higher latitudes

data lying outside this belt. The first fit and the $\pm 2°$-belt are shown by dotted lines in Figure 3. Just as in Brajša *et al.* (2002) and Vršnak *et al.* (2003) the majority of CBPs lies inside a $\pm 2°$-belt so this step of filtering is justified. After this step a new fit presented in Figure 3 (full line) was calculated. We treated both hemispheres together and used absolute values for the solar latitude *b*.

4. Comparing the Results for Rotation

One of the most interesting questions is, whether the result for the rotational angular velocity after data-filtering is still in accordance with other investigations of solar differential rotation done by tracing CBPs. To find the answer we compared the last result with three other observations. These observations were done by three different observers using the interactive method to follow CBPs during October 19 - 29.

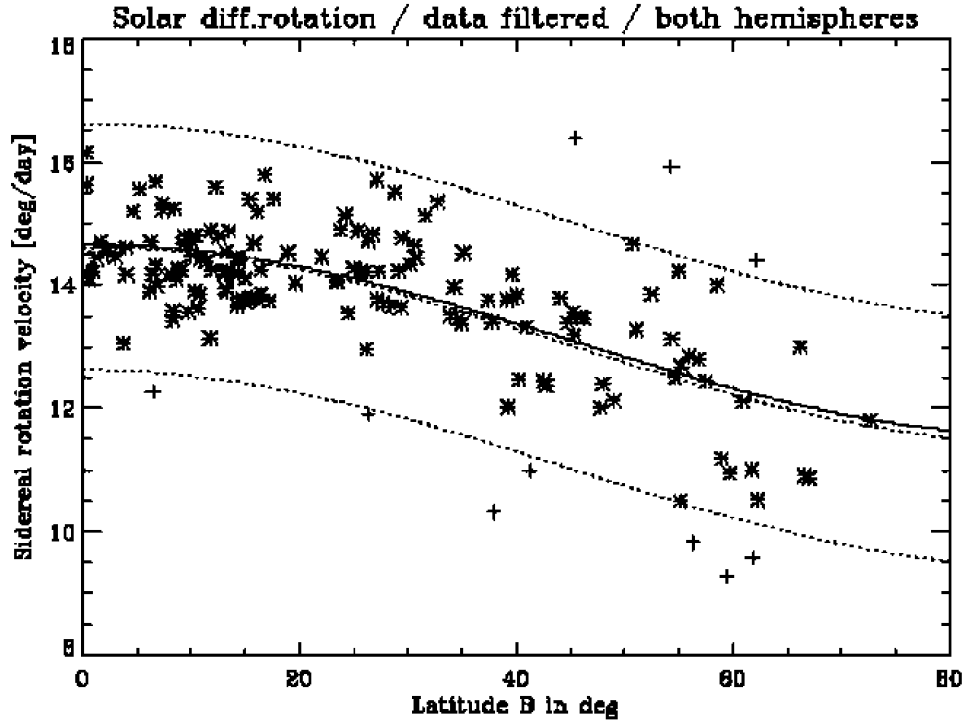After filtering the data the observers calculated three individual fits

Figure 3: Fit for the rotational angular velocity with filtered data in October 1999 (observer M.Mulec). The fit shows a slower solar rotation with increasing latitude *b*. The dotted lines represent the fit after the first filtering and the $\pm 2°$-belt around it. CBPs inside this belt marked by stars were used to get the full line fit.

for the rotational angular velocity. Except a small deviation for the data observed by J.Engler the coefficients are very similar for all observers. Their coefficients and the new result which we present in Figure 3 are compared in Table II.

Except one case where A deviates for nearly 0.68% and B nearly 7.7% towards the last measurement, all coefficients have nearly the same range, the others differ at most 0.2% for A and 1.61% for B.

As the automatic method is less time consuming, the rotational analysis for both data series is already performed. So we were able to compare the interactive results to all results from the automatic method which are listed in Table III. There we can see, that the automatic method picks out much more features declared as ROI than an average interactive observation. Therefore we see, that the values for A differ at most 4% and for B up to 70%.

Table II: Coefficients for the rotational angular velocity-fit for three measurements during 10 days in October 1999 compared to the new measurements over the whole month. n is the number of features used for the individual measurements before and after the particular filtering step.

Observer	A	$-B$	n	Filter	Oct 1999
J. Engler	14.68	2.48	351 335	no 8-18	19-29
	14.76	2.87	297	2nd	
H. Wöhl	14.57	2.74	393 385	no 8-18	19-29
	14.63	3.06	351	2nd	
R. Brajša	14.66	2.61	156 155	no 8-18	19-29
	14.68	3.13	149	2nd	
M. Mulec	14.62	3.19	160 156	no 8-18	all
	14.66	3.11	146	2nd	

5.   Evolution of CBPs

As already mentioned we divide up the CBPs into different types due to their appearance. To calculate their radius we needed a nearly circular shape of the observed CBP; this is the case for PLS and SAR. The interactive observation stores the CBP's size in pixels for each image, so we were able to calculate radius changes in time, for the whole life-periods (Figure 4) and changes in intensity like the ones presented for a SAR. To get better results we had to use another constraint; we took those CBPs, where the effect of visual diameter stretching can be neglected. This is true for CBPs lying inside a box of $\pm 30°$ of b and $\pm 30°$ of CMD. For the new October 1999 observations out of 160 features, 41 remained.

Changes in intensity and radius seem to be directly correlated. So each change in intensity responds to a change in size. This is true especially for SAR as seen in Figure 4; we found intensity increases up to 600%. PLS have not such a direct correlation, but growing PLS show an increase in intensity as well . For SAR and PLS we calculated an average size over the whole time

Table III: Coefficients for the rotational fit calculated for ROI by the automatic method for both data series. n is the number of ROI.

Obs.Period	A	B	Obs.Period	A	B
June 1998	14.51	-3.09	Oct. 1999	14.32	-2.34
Nov. 1998	14.40	-2.73	Nov. 1999	14.35	-2.44
Dec. 1998	14.54	-2.81	Dec. 1999	14.27	-2.38
March 1999	14.57	-3.12	Jan. 2000	14.41	-2.63
April 1999	14.51	-2.40	Feb. 2000	14.40	-2.44
May 1999	14.36	-2.16	Mar. 2000	14.07	-1.49
1998/1999	14.50	-2.72	1999/2000	14.31	-2.32
(n=2960)	$\pm$ 0.02	$\pm$ 0.09	(n=4048)	$\pm$ 0.02	$\pm$ 0.08

of observations. So we receive following results for October 1999, observer M.Mulec :

- PLS 7330km $\pm$ 2422km   SAR 9800km $\pm$ 1318km

By changing it's size a CBP also changes it's type, so very often SAR turn to SL and PLS grow up to SAR, and all possible changes can be observed.

6.   Conclusions

While investigating CBPs in EIT-images and comparing the rotation-fits afterwards, we found that the interactive method turned out to be more accurate. The CBPs could be identified with a higher confidence, whereas the automatic method picks out a larger number of features declared as ROI. The automatic method works much faster and the physical observers do not have to pick out the desired structures (Brajša *et al.*, 2001). For studying the individual point's evolution, the interactive method is more convenient because of the possibility to separate the CBPs into different types, where the automatic method recognizes only ROI.

The interactive results show nearly the same values for the rotation coefficients and vary in a very small range. Results for the automatic method deviate a bit more from the last measurements made by M.Mulec for October 1999. The reasons are the individual identifications and observations of

8

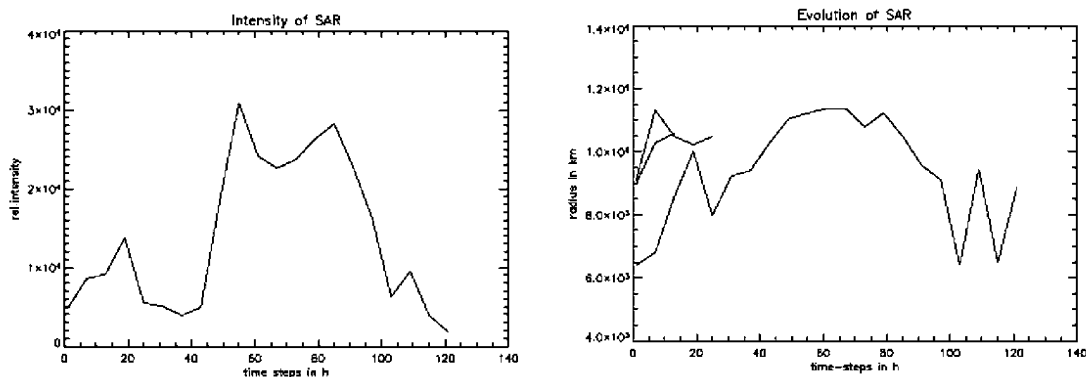*Cent. Eur. Astrophys. Bull.* **31** (2007) 1, 1–10

Figure 4: left: Evolution of SAR in relative intensity towards the background of the Corona in Fe XV emission line. According to the right plot, where for three SAR the whole evolution in growth can be followed. The long living SAR in the right plot is the same SAR as in the left plot.

CBPs which affect the interactive method and the higher number of used features for the automatic method. As the rotation velocity shows nearly the same value, the differences are not really significant; the parameter B is connected to the $\sin^2(b)$ term so even a deviation of 70% for B does not really make a large difference for the whole fit where the parameter A has a dominant role, and for A all the deviations are small.

The changes of intensity are directly correlated for SAR where we observed changes up to 600%. The intensity-size correlation for PLS is more complicated, but even here a growth causes an increase in intensity. The SAR turned out to be a little larger than the PLS, and the dimensions of the SL's lie somewhere in between.

Acknowledgements

References

Brajša, R., Wöhl, H., Vršnak, B., Ruždjak, V., Clette, F., and Hochedez, J. F.: 2001, *Astron. Astrophys.* **374**, 309.

Brajša, R., Wöhl, H., Vršnak, B., Ruždjak, V., Clette, F., and Hochedez, J. F.: 2002, *Astron. Astrophys.* **392**, 329.

Vršnak, B., Brajša, R., Wöhl, H., Ruždjak, V., Clette, F., and Hochedez, J. F.: 2003, *Astron. Astrophys.* **404**, 1117.

Wöhl, H., Brajša, R., Vršnak, B., Ruždjak, V., Clette, F., and Hochedez, J. F.: 2001, *Hvar Obs. Bull.* **25**, 27.